Supporting Information

Size-Tailored and Acid-Degradable Polyvinyl Alcohol Microgels for Inhalation Therapy of Bacterial Pneumonia

Xiang Zhou [a,1], Jingjing Zhou [a,1], Lanlan Wang [a], Bingbing Zhao [a, *], Yukun Ma [a], Ni Zhang [a], Wei Chen [a, b, *], Dechun Huang [a, b, *]

[a] *Department of Pharmaceutical Engineering, School of Engineering, China Pharmaceutical University, Nanjing 210009, China*

[b] *Engineering Research Center for Smart Pharmaceutical Manufacturing Technologies, Ministry of Education, School of Engineering, China Pharmaceutical University, Nanjing 211198, China*

[*] Corresponding authors

E-mail address:

zhaobb@cpu.edu.cn (BB. Zhao)

w.chen@cpu.edu.cn (W. Chen)

cpuhdc@cpu.edu.cn (DC. Huang)

[1] These authors contributed equally to this work

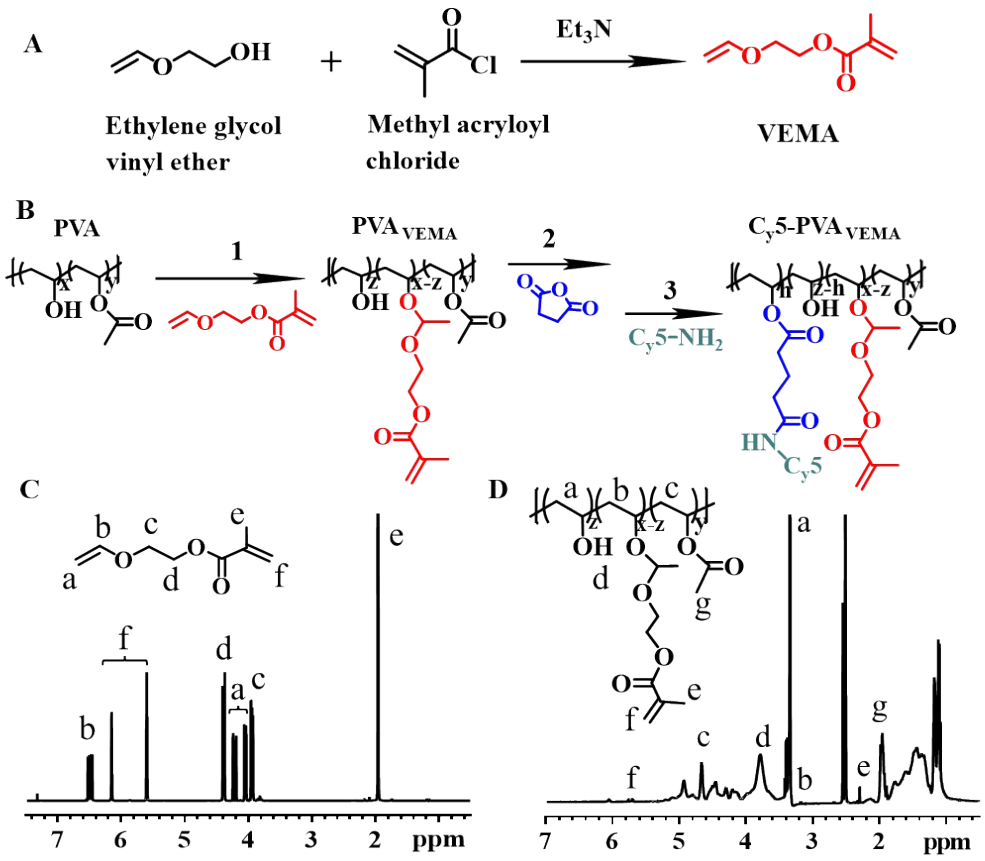

Figure S1. Preparation and characterization and of VEMA, PVA_{VEMA} and Cy5-PVA_{VEMA}. (A) Synthesis steps of VEMA. (B) Synthesis steps of PVA_{VEMA} and Cy5-PVA_{VEMA}. (C) ^1H NMR spectra of VEMA (400 MHz, $CDCl_3$). (D) ^1H NMR spectra of PVA_{VEMA} (400 MHz, DMSO-*d6*).

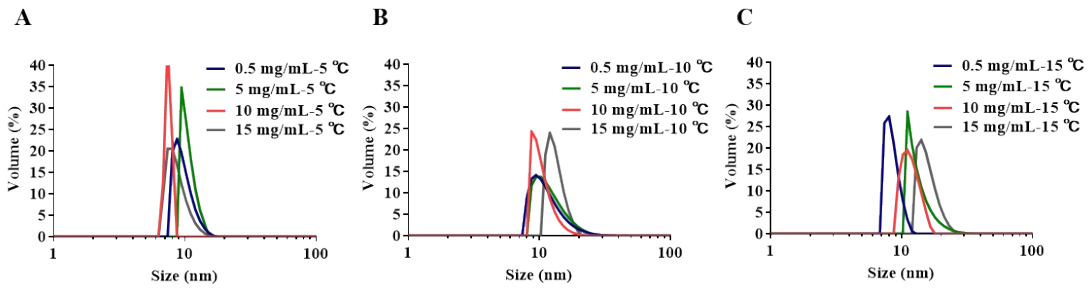

Figure S2. Size distribution of PVA_{VEMA} dispersed in water at various concentrations and at 5 °C (A), 10 °C (B) and 15 °C (C).

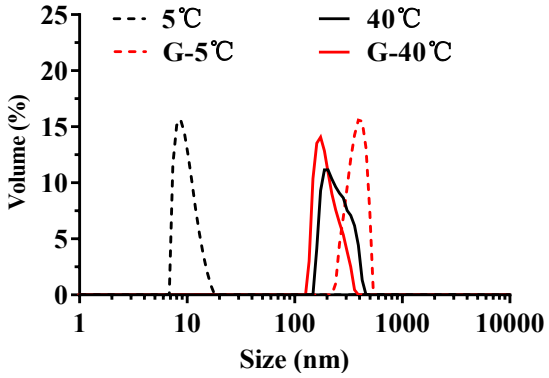

Figure S3. Particle size distribution of 0.5 mg/mL aqueous solution of PVA_{VEMA} aggregation and PVA_{VEMA} microgels (G) at 5 and 40°C. (Cross-linked: red dashed line, uncross-linked: black dashed line)

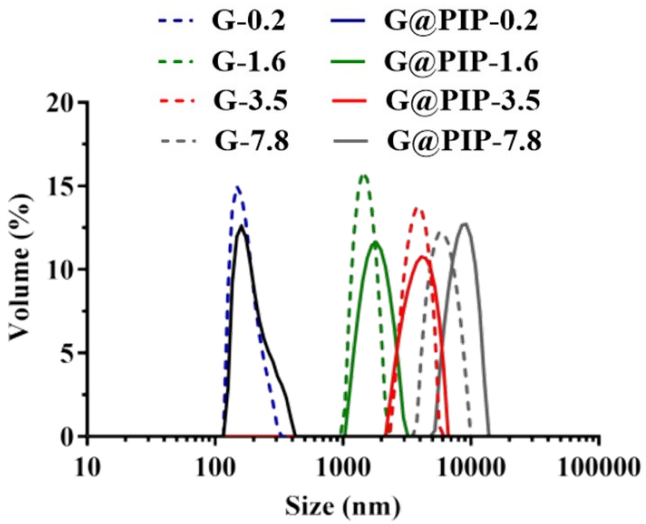

Figure S4. Size distribution of the PVA $_{VEMA}$ microgels before and after loading with PIP. (Before loading: red dashed line, After loading: solid line)

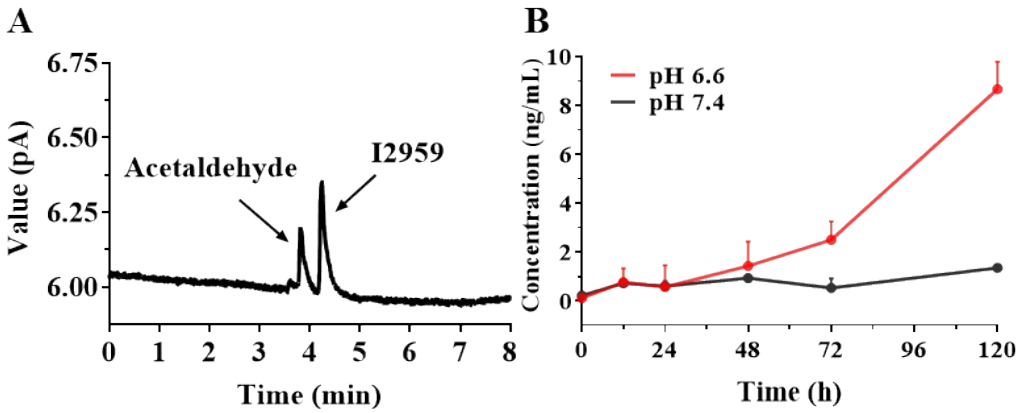

Figure S5. The pH degradation of PVA_{VEMA} microgel. (A) Gas chromatographic detection of PVA_{VEMA} microgel after complete degradation under acidic conditions. (B) Gas chromatographic detection of degradation of PVA_{VEMA} microgel at pH 7.4 and 6.6 for 120 h.

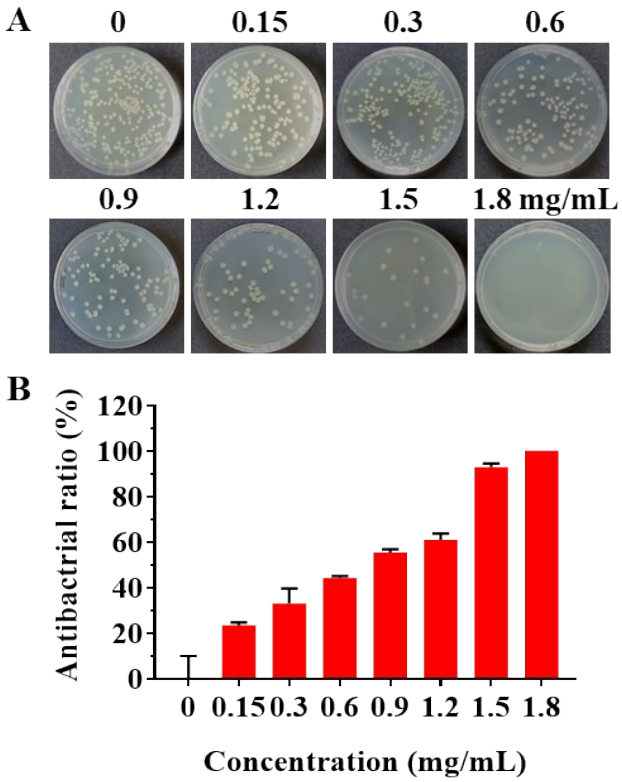

Figure S6. Antibacterial activity of the antibiotic drug PIP *in vitro*. (A) Coated plate method to evaluate the effect of different concentrations of PIP on *E. coli-lux* inhibition (A) and corresponding statistics (B). All data are presented as the mean ± SD (n = 3).

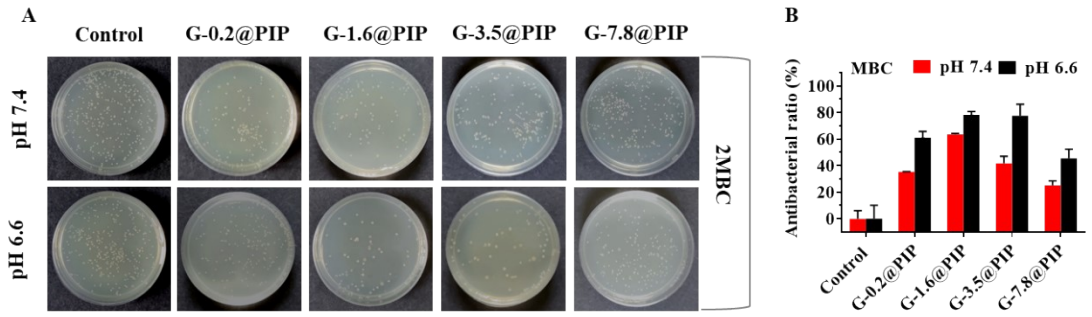

Figure S7. *In vitro* analysis of antibacterial properties. (A) Changes in colony growth of *E. coli-lux* with different groups (Control, G-0.2@PIP, G-1.6@PIP, G-3.5@PIP and G-7.8@PIP, PIP: 1.8 mg mL^{-1}, MBC) incubated under pH 7.4 and pH 6.6 conditions. Survival statistics of the corresponding bacteria under conditions (B). All data are presented as the mean ± SD (n = 3).

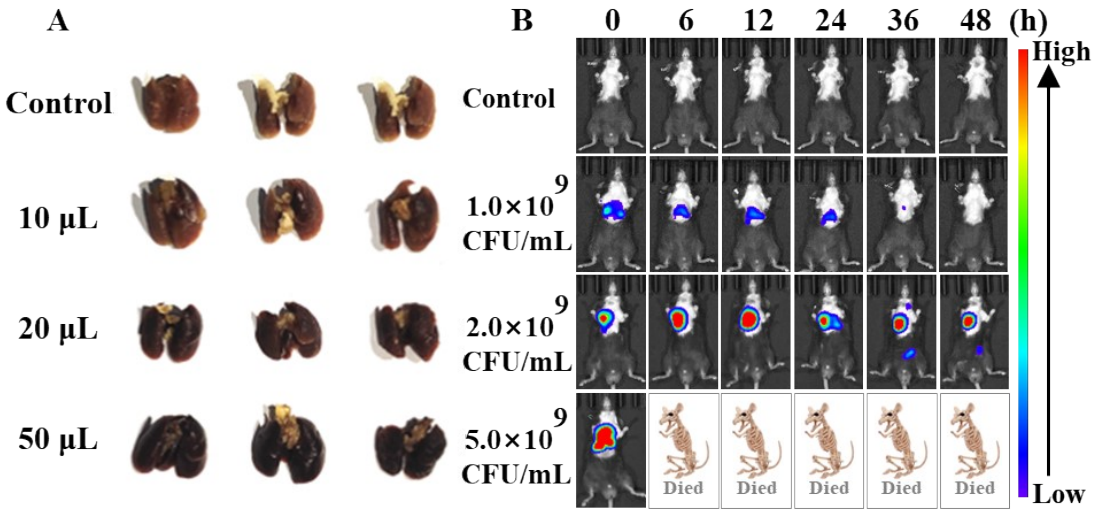

Figure S8. Modeling of pneumonia. (A) *In vitro* photograph of isolated lung organs 48 h after injection of different volumes of *E. coli-lux* solution into the right lung parenchyma. (B) Photographs of fluorescence imaging of living mice at the indicated time points after injection of *E. coli-lux* solutions (10 μL/mouse) into the right lung parenchyma. All data are presented as the mean ± SD (n = 3).